

© MICROSCOPY SOCIETY OF AMERICA 2016

# Collagen Fibril Ultrastructure in Mice Lacking Discoidin Domain Receptor 1

Jeffrey R. Tonniges, <sup>1</sup> Benjamin Albert, <sup>2</sup> Edward P. Calomeni, <sup>3</sup> Shuvro Roy, <sup>4</sup> Joan Lee, <sup>4</sup> Xiaokui Mo, <sup>5</sup> Susan E. Cole, <sup>6</sup> and Gunjan Agarwal <sup>2,4,\*</sup>

**Abstract:** The quantity and quality of collagen fibrils in the extracellular matrix (ECM) have a pivotal role in dictating biological processes. Several collagen-binding proteins (CBPs) are known to modulate collagen deposition and fibril diameter. However, limited studies exist on alterations in the fibril ultrastructure by CBPs. In this study, we elucidate how the collagen receptor, discoidin domain receptor 1 (DDR1) regulates the collagen content and ultrastructure in the adventitia of DDR1 knock-out (KO) mice. DDR1 KO mice exhibit increased collagen deposition as observed using Masson's trichrome. Collagen ultrastructure was evaluated *in situ* using transmission electron microscopy, scanning electron microscopy, and atomic force microscopy. Although the mean fibril diameter was not significantly different, DDR1 KO mice had a higher percentage of fibrils with larger diameter compared with their wild-type littermates. No significant differences were observed in the length of D-periods. In addition, collagen fibrils from DDR1 KO mice exhibited a small, but statistically significant, increase in the depth of the fibril D-periods. Consistent with these observations, a reduction in the depth of D-periods was observed in collagen fibrils reconstituted with recombinant DDR1-Fc. Our results elucidate how DDR1 modulates collagen fibril ultrastructure *in vivo*, which may have important consequences in the functional role(s) of the underlying ECM.

Key words: collagen, aorta, discoidin domain receptor 1, electron microscopy, atomic force microscopy

# Introduction

Collagen type I fibrils are the major constituent of the extracellular matrix (ECM) present in connective tissues. The quantity, organization, and structure of collagen fibrils play an important role in dictating ECM remodeling (Manabe et al., 2002; Fomovsky et al., 2012), cell-matrix interactions (Bhatnagar et al., 1997; Orgel et al., 2011), and mechanical properties (Chen et al., 2011; Ghazanfari & Driessen-Mol, 2012; Cheng & Stoilov, 2013; Sugita & Matsumoto, 2013) of the underlying tissue. Collagen content in the ECM is regulated by a number of factors, including the expression of collagen-binding proteins (CBPs) that possess the ability to regulate collagen fibrillogenesis. A number of studies employing knock-out (KO) mouse models have elucidated the role of CBPs secreted in the ECM in regulating collagen deposition and fibril diameter (Table 1). However, very little is understood on how the collagen fibril ultrastructure (e.g., the D-periodicity) is affected by these soluble CBPs. Even less is known regarding the ability of cell-surface collagen receptors to regulate collagen

deposition and ultrastructure *in vivo*. This is especially important as the past decade has provided two novel insights into the putative role of CBPs in regulating collagen fibrillogenesis, namely (i) the binding sites of several CBPs have been mapped onto the collagen type I triple helix (Farndale et al., 2008; Sweeney et al., 2008) and (ii) the packing of collagen molecules in the gap and overlap zones of the D-period and the arrangement of the microfibril in the type I collagen fibril has been revealed using X-ray diffraction (Orgel et al., 2006; Herr & Farndale, 2009). Thus, binding of CBPs at specific sites on the collagen triple helix could perturb the packing of collagen molecules, which could be manifested as alterations in the length or depth of D-periods in the fibril.

The CBP discoidin domain receptor 1 (DDR1) is a widely expressed receptor tyrosine kinase, which binds to and is activated by collagens, including types I–III (Shrivastava et al., 1997; Vogel et al., 1997). The extracellular domain (ECD) of DDR1 is necessary and sufficient for collagen binding (Vogel et al., 1997). Recently, the DDR1 binding site on the collagen type III triple helix has been identified (Xu et al., 2011) and mapped to lie in the gap region of the collagen type I fibril. The DDR1 ECD is also shed as a soluble protein in the ECM in various cell types

<sup>&</sup>lt;sup>1</sup>Biophysics Graduate Program, The Ohio State University, Columbus, OH 43210, USA

<sup>&</sup>lt;sup>2</sup>Biomedical Engineering Department, The Ohio State University, Columbus, OH 43210, USA

<sup>&</sup>lt;sup>3</sup>Department of Pathology, The Ohio State University, Columbus, OH 43210, USA

<sup>&</sup>lt;sup>4</sup>David Heart and Lung Research Institute, The Ohio State University, Columbus, OH 43210, USA

<sup>&</sup>lt;sup>5</sup>Center for Biostatistics, The Ohio State University, Columbus, OH 43210, USA

<sup>&</sup>lt;sup>6</sup>Department of Molecular Genetics, The Ohio State University, Columbus, OH 43210, USA

Table 1. Regulation of Collagen Fibrillogenesis in Mice Lacking a Collagen-Binding Protein (CBP).

CBP	Tissue(s)	Collagen Deposition	Fibril Diameter	References
Decorin	Skin	_	Irregular	Danielson et al. (1997)
Lumican	Skin, heart, cornea	Reduced	Increased	Chakravarti et al. (1998), Dupuis et al. (2015), Chakravarti et al. (2000)
Fibromodulin	Tendon, skin	Reduced	Irregular and decreased	Svensson et al. (1999), Jepsen et al. (2002)
SPARC	Heart, skin	Reduced	Decreased	Rentz et al. (2007), Bradshaw et al. (2003, 2010)
Thrombospondin2	Tendon, skin	Reduced	Irregular and increased	Kyriakides et al. (1998)
Periostin	Skin	Reduced	Decreased	Norris et al. (2007)
Biglycan	Tendon	_	Decreased	Ameye et al. (2002)

Comparisons have been made between the CBP knock-out mice relative to their wild-type littermates. SPARC, secreted protein acidic and rich in cysteine.

(Vogel, 2002; Slack et al., 2006; Fu et al., 2013), but the collagen-binding activity of the shed fragment has not yet been elucidated. In our earlier in vitro studies, we demonstrated that the presence of DDR1 ECD as a recombinant (Agarwal et al., 2007) or cell-secreted protein (Blissett et al., 2009; Flynn et al., 2010) altered collagen fibrillogenesis and resulted in fibrils with a weakened D-periodicity when examined using transmission electron microscopy (TEM). DDR1 ECD secretion by cells also led to decreased collagen deposition and fibrils with thinner diameters. In vivo, limited studies exist on collagen regulation by DDR1. DDR1 KO mice have poorly developed mammary glands with increased collagen deposition (Vogel et al., 2001). In a mouse model for atherosclerosis, DDR1 KO mice exhibited fewer and smaller plaques with proportionally more collagen deposition than wild-type (WT) mice (Franco et al., 2008, 2009, 2010). Despite these observations, collagen ultrastructure in the ECM of DDR1 KO mice remains uncharacterized.

In this study, we investigated how deletion of DDR1 impacts collagen content and ultrastructure *in vivo*. We focused our studies on the murine vascular adventitia, which is rich in collagen type I (Hechler et al., 2010) and contains DDR1, expressed in the adventitial fibroblasts (Hou et al., 2001). Aortas from mice deficient in DDR1 were dissected, analyzed, and compared with their WT littermates. Histological staining, as well as electron and atomic force microscopy (AFM) techniques, were used to characterize the collagen content and the fibril D-periods in the adventitia. Our studies provide novel insights into how DDR1 modulates collagen deposition and fibril ultrastructure in the aortic wall.

## MATERIALS AND METHODS

## Animals

DDR1 KO mice, used in this study were generated by Lexicon Pharmaceuticals Inc. (Woodlands, TX, USA) using homologous recombination. Coding exons 1–3 of the DDR1 gene were replaced with the LacZ/Neo3a cassette (Fig. 1a) resulting in silencing of the DDR1 gene (NCBI accession NM\_007584). Heterozygous mice with a 129Sv/C57BL6 background, thus generated, were purchased through the Texas Institute of Genomic Medicine. DDR1 KO mice and

their WT littermates were obtained through heterozygous breeding at expected Mendelian frequency. Animal studies were performed according to a protocol approved by the Institutional Animal Care and Use Committee at the Ohio State University. Studies were performed on 6–8-month-old DDR1 KO mice and their age- and gender-matched WT littermates. Murine tissue was processed and analyzed in sets of WT/KO littermate pairs.

## Genotyping

Mice were genotyped by polymerase chain reaction (PCR) to determine the presence of the DDR1 and/or the Neo3a (mutant) allele. At weaning, tail clippings were lysed in direct PCR lysis buffer (Viagen Biotech, Los Angeles, CA, USA) and used as a template for PCR. The primer sequences are shown in Table 2. The PCR conditions were 95 °C for 4 min, followed by 35 cycles at 95 °C for 30 s, 59 °C for 30 s, and 72 °C for 30 s. Cycling was followed by a final extension step at 72 °C for 7 min. WT, homozygous DDR1<sup>-/-</sup>, and heterozygous DDR1<sup>+/-</sup> mice were identified by the presence of DDR1, Neo3, or both the PCR products, respectively (Fig. 1a). Mice used in this study were re-genotyped upon euthanasia to confirm their genotype.

As an additional verification of genotype and to confirm successful insertion of the LacZ/Neo3a cassette into the DDR1 KO mouse,  $\beta$ -galactosidase expression was examined with x-gal staining. Brain, heart, aorta, and skin (from the upper back) were dissected from WT and KO mice and subjected to  $\beta$ -galactosidase staining as follows (Williams et al., 2014). Tissues were fixed in 1% paraformaldehyde, 0.2% glutaraldehyde, 2 mM MgCl<sub>2</sub>, 5 mM EGTA (ethylene glycol tetraacetic acid), and 0.02% IGEPAL (IGEPAL® CA-630) CA-630 (Sigma-Aldrich, St. Louis, MO, USA). After washing in 0.02% IGEPAL, tissues were stained with x-gal solution [1 mg/ml x-gal,  $5 \text{ mM} \text{ K}_3\text{Fe}(\text{CN})_6$ ,  $5 \text{ mM} \text{ K}_4\text{Fe}(\text{CN})_6$ ,  $2 \text{ mM} \text{ MgCl}_2$ , 0.01% deoxycholic acid, 0.02% IGEPAL] for 2 weeks at 4°C. The tissue pieces were thereafter rinsed in ethanol and imaged using light microscopy. Strong x-gal staining was observed in the brain, heart, and skin of the DDR1 KO mice, but not in the WT tissues (Fig. 1b). Small punctate x-gal staining was observed in DDR1 KO aortas, whereas no staining was observed in WT aortas.

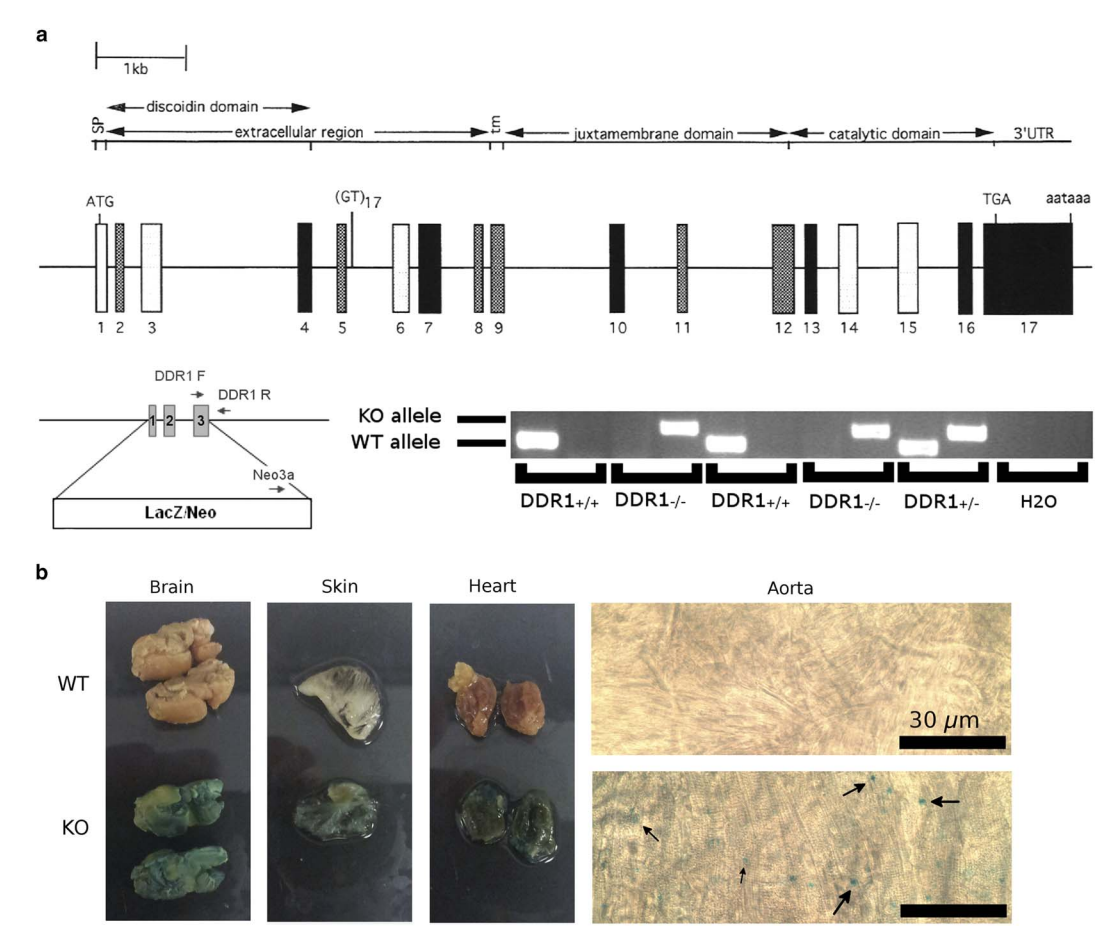


Figure 1. Genotyping of discoidin domain receptor 1 (DDR1) knock-out (KO) mice. a: Schematic shows generation of the DDR1 KO mouse through homologous recombination, by replacing exons 1-3 with a LacZ/Neo cassette. The genotype of the mice was determined using polymerase chain reaction of tail lysates. Presence of DDR1, Neo3a, or both alleles indicated homozygous positive (DDR1<sup>+/+</sup>), homozygous negative (DDR1<sup>-/-</sup>), and heterozygous (DDR1<sup>+/-</sup>) mice, respectively. b: Brain, skin, and heart extracted from DDR1 KO mice exhibited strong x-gal staining, whereas wild-type (WT) tissues did not. The brain and heart have been cut in half to illustrate staining. Aortic longitudinal sections, viewed with white light microscopy from the luminal side, revealed punctate x-gal staining in DDR1 KO aortas (black arrows), whereas no staining was observed in WT aortas. Scale bar is  $30 \,\mu\text{m}$ .

## **Aorta Extraction**

Thoracic aortas were dissected from male and female mice within 30 min of death. Excision of the aortas was initiated just distal to the left subclavian artery and terminated at the diaphragm. The dissected aortas were cut into portions and immediately stored for experiments as detailed below. For each mouse, the same region was allocated for the same experiment, namely the ~2 mm most proximal region was used for TEM analysis, the next ~2 mm region was used for Trichrome staining, and the rest of the excised aorta was used for scanning electron microscopy (SEM) and AFM analysis.

#### Masson's Trichrome Staining

Portions from the dissected aortas were fixed in 10% neutral-buffered formalin for at least 24 h, paraffin embedded, and stained with Masson's trichrome. Trichrome-stained specimens were imaged using a 40×

objective. Images were analyzed using ImageJ software (NIH). Thickness of the adventitial layer was determined by crude integration, i.e., by measuring the area of the layer and dividing by the length of the midline of the layer. Measurements were calibrated using a stage micrometer (2280-16, Ted Pella, Redding, CA, USA). Adventitial thickness was determined only from intact contiguous adventitia, which was often surrounded by adjacent intact tissue. Aorta sections where the adventitia appeared to be falling apart or diffuse in staining were excluded from our analysis. The mean adventitial thickness was determined using at least three images from each mouse. The number of mice  $(n_{\rm m})$ analyzed and the mean adventitial thickness obtained for each genotype are summarized in Table 3.

### **TEM**

Portions from the dissected aortas were fixed in 4% buffered glutaraldehyde for at least 24 h and thereafter processed for TEM (Blissett et al., 2009; Flynn et al., 2010). Briefly, specimens were post-fixed in 1% osmium tetroxide and en-bloc stained with a saturated aqueous uranyl acetate solution. Thereafter, specimens were dehydrated in a graded ethanol series and then embedded in Spurr's epoxy resin (Electron Microscopy Sciences, Fort Washington, PA, USA). Tissue blocks were sectioned with a Leica Ultracut UCT ultramicrotome (Leica Microsystems GmbH, Wien, Austria). Electron micrographs were generated using a JEOL JEM-1400 TEM (JEOL Ltd. Tokyo, Japan) equipped with a Veleta digital camera (Olympus Soft Imaging Solutions GmbH, Műnster, Germany). Images were calibrated with a grating replica calibration grid with parallel lines (Electron Microscopy Services).

Collagen fibril diameters were determined by measuring the length of the shortest diameter of collagen cross-sections using ImageJ (NIH). The mean fibril diameter for each mouse was ascertained by averaging at least 800 fibrils. A MATLAB code was used to fit the collagen diameter distributions to a Gaussian function and the full-width at half-maxima (FWHM) for each mouse was determined. We also classified fibrils into categories according to their diameter ranges (0–25, 25–50, etc.) and ascertained the average number of fibrils in each range across  $n_{\rm m}=8$  mice of each genotype. We then used a  $\chi^2$  test to determine if there was a difference in the percentage of fibrils with

Table 2. Primer Sequences Used for Genotyping Litters.

m	n		Predicted PCR Product
Target	Primer	Sequence (5′–3′ Direction)	Size (bp)
DDR1	Forward	GTTGCGTTACTCCCGAGATG	159
	Reverse	AGACAATCTCGAGATGCTGG	
Neo3a	Forward	GCAGCGCATAGCCTTCTATC	243
cassettea	Reverse	AGACAATCTCGAGATGCTGG	

<sup>&</sup>lt;sup>a</sup>Primers target sequence containing portion of the inserted Neo3a cassette and discoidin domain receptor 1 (DDR1).

diameters >50 nm between the two genotypes. Data were analyzed by using Minitab software 16 (Minitab, State College, PA, USA).

Longitudinal regions of the adventitial collagen fibrils were analyzed for length of D-periods, which was measured perpendicular to the bands using ImageJ. The length of the D-period for each fibril was determined by averaging at least four D-periods along the fibril axis and the mean D-length per mouse was determined by averaging values from at least 15 fibrils. The length of individual gap and overlap regions were also independently measured in a subset of fibrils from each mouse. The number of mice  $(n_{\rm m})$ , total number of fibrils  $(n_{\rm f})$  analyzed, and mean values for fibril diameter and length of D-periods for each genotype are summarized in Table 3.

#### **SEM**

Dissected aortas were cleaned of perivascular adipose tissue and embedded in optimal cutting temperature (OCT) compound by flash freezing in liquid nitrogen. Five- $\mu$ m thick sections were cryosectioned, adhered to poly-lysine-coated (EMD Millipore, Billerica, MA, USA) glass coverslips, and stored at -20 °C until use. The aortic sections were washed three times with phosphate-buffered saline (PBS), fixed with 2% glutaraldehyde, washed three times with PBS, washed two times with ultrapure water, and incubated in ultrapure water for 1h to ensure removal of OCT residue. Sections were dehydrated by air drying in a vacuum desiccator at room temperature overnight and thereafter coated with gold-palladium for 40 s in a Cressington 108 sputter coater (Cressington, Watford, England). The coated aortic sections were imaged using the through-the-lens detector of a FEI Nova NanoSEM 400 (FEI, Hillsboro, Oregon, USA) SEM with an accelerating voltage of 5 kV. The length of D-periods in the longitudinal images of collagen fibrils was measured using ImageJ. D-period lengths were determined by averaging at least five periods in a fibril and also by measuring individual D-periods in each fibril. At least, n = 20 fibrils were analyzed per mouse. The number of mice  $(n_{\rm m})$ , total

Table 3. Summary of Measurements of Various Parameters in the Adventitial Collagen in Murine Aorta.

	Fibril Diameter (nm)  Adventitia [Average]  Thickness (µm) [(FWHM)]		TEM	SEM	AFM	Depth of D-Period (nm)
DDR1 KO WT	-	56.6 ± 7.3 (8; 9047) Measured per 52.3 ± 8.7 (8; 8822) fibril	r $46.6 \pm 2.3$ (8; 198) $48.6 \pm 1.0$ (8; 219)	_ , ,	,	$3.6 \pm 0.6 (8; 43)$ $3.0 \pm 0.4 (8; 42)$
DDR1 KO WT	$37.2 \pm 1.2$ (6) $26.8 \pm 5.1$ (6)	18.2 ± 4.7 (8; 9047) Measured po 18.1 ± 3.4 (8; 8822) D-period	r $46.6 \pm 2.1$ (8; 1188) $48.5 \pm 0.6$ (8; 1314)			

Means  $\pm$  SD are listed with number of mice  $(n_{\rm m})$  and number of collagen fibrils  $(n_{\rm f})$ , or number of D-periods  $(n_{\rm p})$  in parentheses  $(n_{\rm m}; n_{\rm f} \text{ or } n_{\rm p})$ . Shaded cells = means are statistically significant (p < 0.05).

FWHM, full-width at half-maxima; TEM, transmission electron microscopy; SEM, scanning electron microscopy; AFM, atomic force microscopy; DDR1, discoidin domain receptor 1; KO, knock-out; WT, wild-type.

PCR, polymerase chain reaction.

number of fibrils ( $n_f$ ) analyzed, and mean values for length of D-periods for each genotype are summarized in Table 3.

#### **AFM**

Aortic sections were prepared as described for SEM but used without the metal coating. AFM imaging was performed using the Multimode AFM equipped with a JV scanner and a Nanoscope IIIa controller (Bruker Inc., Santa Barbara, CA, USA). A reflected light module mounted over the AFM head enabled laser alignment on the AFM probe and visualization of the aortic section for AFM imaging. The adventitial and medial regions could be easily distinguished using this module. AFM imaging was performed in tapping mode in ambient air using NSC15 cantilevers (Micromasch, Estonia) with a nominal spring constant of 40 N/m. Both height and amplitude images were recorded at 512 lines/scan direction with a scan speed of two lines per second and at a scan angle of 0 degrees.

AFM probes were characterized for tip radius (Fig. S1) by ascertaining the estimated tip diameter (ETD1) at a height of 5 nm from the apex by using the tip-estimation module and a polycrystalline titanium roughness sample available on the Bioscope Resolve AFM equipped with a Nanoscope V controller (Bruker Inc.). Our probes had an ETD1 range of 10-23 nm with an average value of  $16.7\pm5.6$  nm and an aspect ratio of  $0.91\pm0.16$ . The same AFM probe was typically used to image sections from each KO/WT pair. Interprobe variability was examined by testing three different probes on the same region of the sample.

The length and depth of D-periodicity of collagen fibrils in the adventitia were measured from AFM topographic images using the WSxM software (Horcas et al., 2007). Only fibrils oriented at identical angles ( $\pm 15^{\circ}$ ) in AFM images of each KO/WT pair were selected for analysis. The length and depth of individual D-periods were ascertained by geometric analysis as shown in Figure 2. At least five periods per fibril and five fibrils per mouse were included in our analysis. The length of D-period per fibril was also measured by one-dimensional Fourier transform on the AFM amplitude images, namely by manually tracing a line perpendicular to the fibril bands and measuring the power spectrum density. The number of mice ( $n_{\rm m}$ ) and number of fibrils ( $n_{\rm f}$ ) analyzed using AFM are summarized in Table 3.

#### In Vitro Reconstituted Collagen

Collagen type I fibrils were reconstituted *in vitro* by incubating monomeric collagen in neutral buffer conditions at 37 °C for 24 h in the presence or absence of recombinant DDR1-Fc protein as previously described (Agarwal et al., 2007). The source of collagen monomers was PurCol collagen I (Advanced BioMatrix, San Diego, CA, USA), and DDR1-Fc fusion protein was purchased (R&D Systems, Minneapolis, MN, USA). The collagen fibrils, thus formed, were immobilized on freshly cleaved mica, washed with water, air-dried, and subjected to AFM imaging and analysis.

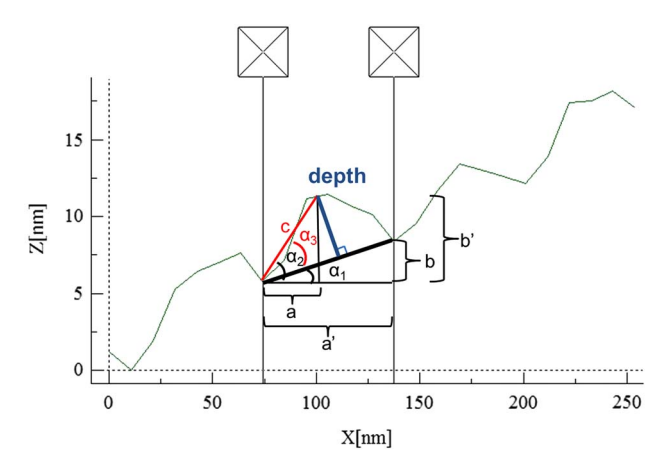


**Figure 2.** Schematic illustrating geometric analysis of collagen fibril profiles from atomic force microscopy height images to determine the length and depth of D-periodicity. This geometric analysis accounts for fibril inclinations departing from the horizontal plane. The lengths (a', b', and a, b) and angles  $(\alpha_1, \alpha_2)$ , corresponding to the width and height of an individual D-period were directly measured using WSxM software. The segment c and angle,  $\alpha_3$ , in red were calculated. The length of a D-period (bold black line) was calculated using a and  $\cos\alpha_1$ . The D-period depth (bold blue line) was defined as the line perpendicular to D-period length and extending up to the highest point in the profile for the overlap. The depth was calculated as c sin  $\alpha_3$ .

# **Statistical Analysis**

The results for each parameter (adventitial thickness, fibril diameter, FWHM, D-length, and D-depth) measured are summarized in Table 3 and by box and whisker plots indicating the overall mean, median, and percentiles (25 and 75%) for each genotype. The Student's two-tailed t-test for paired data was performed using Excel to determine statistical significance between the two genotypes. For all t-tests, approximate p-values are given, and a p-value < 0.05 was considered statistically significant.

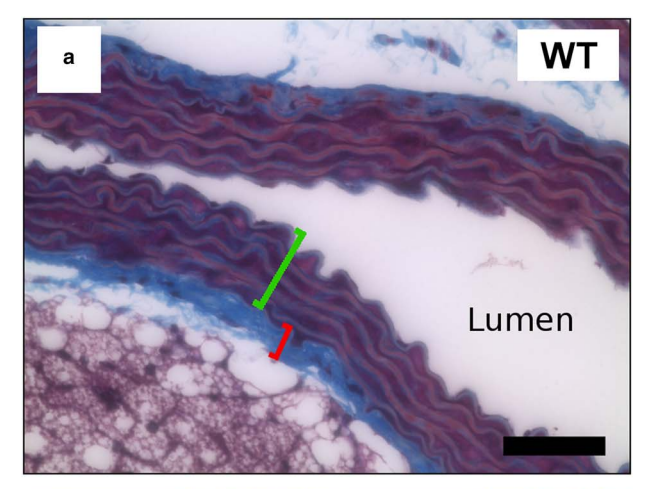
# Results

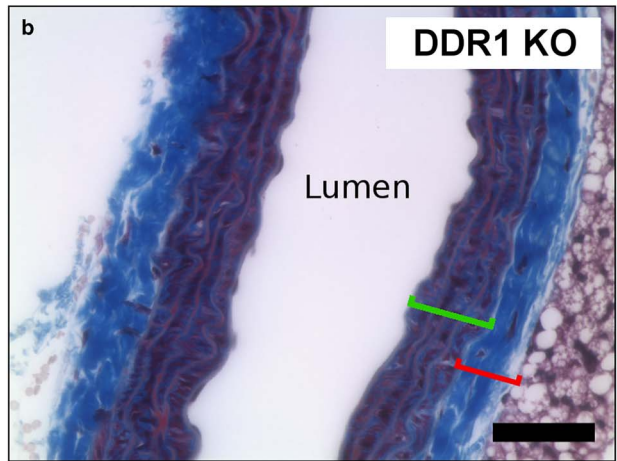
## Effect of DDR1 on Collagen Deposition

Descending thoracic aortas were fixed, paraffin embedded, sectioned, and stained with Masson's trichrome. Collagen was observed as a near-contiguous blue staining in the adventitia and as interspersed blue staining between the elastic lamellae and smooth muscle cells in the media (Figs. 3a, 3b). The thickness of the adventitial collagen layer was significantly greater in DDR1 KO mice as compared with WT (Fig. 3c; p = 0.039; Table 3). No significant difference in the thickness of the media was observed between the two genotypes (data not shown). The thicker adventitia in DDR1 KO aortas indicates an increased collagen deposition.

### Effect of DDR1 on Collagen Fibril Diameter

Collagen fibril diameters were measured from fibril crosssections in TEM images. The majority of the adventitial layer





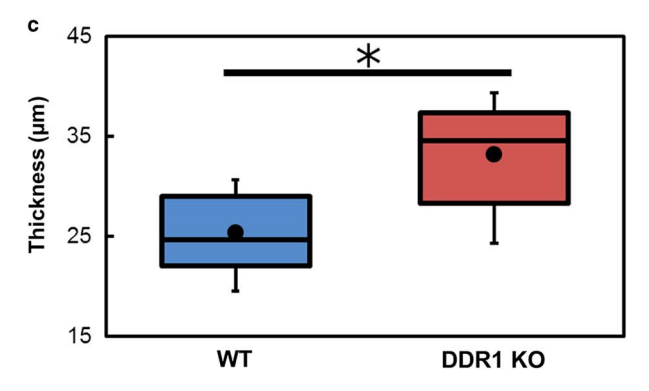


Figure 3. Deletion of discoidin domain receptor 1 (DDR1) enhanced collagen deposition in aortic adventitia. Masson's trichrome staining shows adventitial collagen (blue stain) in the thoracic aorta from (a) wild-type (WT) and (b) DDR1 knock-out (KO) mice. Brackets indicate the adventitial (red) and medial (green) layers. c: The mean adventitial thickness for each genotype is displayed in boxplots. Average of the means is indicated by a dot. The adventitial thickness for DDR1 KO aortas was significantly greater than the WT (p = 0.039). Scale bar is  $100 \,\mu\text{m}$ .

contained fibrils with circular cross-sections and relatively homogeneous diameter distributions (Figs. 4a, 4b). Both genotypes exhibited a subpopulation of larger and sometimes irregular cross-sections of collagen fibrils (Figs. 4c, 4d). These regions were generally observed near the interface of the media and adventitia and made up <10% of collagen fibrils analyzed. Quantitative analysis revealed that the mean collagen fibril diameter was larger in DDR1 KO as compared with WT littermates, but the difference was not statistically significant (p = 0.236; Table 3). We also fit the frequency distributions for collagen fibril diameters to a Gaussian curve and ascertained the FWHM for each mouse. No significant difference was observed between the FWHMs of the two genotypes (p = 0.95; Table 3). However, when we fit the frequency distribution of the entire genotype to a Gaussian curve, the DDR1 KO mice exhibited a narrower distribution of fibril diameters compared with WT (data not shown) and also a greater subpopulation of large (>75 nm) diameter fibrils compared with WT. To evaluate whether differences in fibril diameter distribution correlated with genotype, the fibrils were classified into two groups according to diameter (< or >50 nm) (Fig. 4e). The percent of fibrils with a size of >50 nm in the DDR1 KO mice was 69%, whereas that in the WT group was 56%. The KO mice had 13% more fibrils with a size of >50 nm, and a  $\chi^2$  test showed that this difference was significant (p < 0.0001).

# Effect of DDR1 on the Length of D-Period

D-period length in the collagen fibrils in the adventitia was evaluated by AFM, SEM, and TEM imaging. The characteristic D-period bands were exhibited in both genotypes (Fig. 5). The mean values of D-period length per fibril, determined via each imaging modality are shown as boxplots and are also listed in Table 3. The length of D-periods determined by TEM was significantly lower as compared with AFM and SEM measurements. However, no significant differences in the length of D-periods were observed between the two genotypes using any of the imaging techniques. Measurements of the length of individual D-periods versus that per fibril also revealed no significant differences among the two genotypes (Table 3), except for the smaller TEM measurements (p = 0.045).

# Effect of DDR1 on the Depth of D-Period

As another unique feature of the collagen ultrastructure, the depth of the gap region ("groove") in a D-period along the collagen fibril was measured from AFM height images (Fig. 6). The average depth of the D-period in DDR1 KO  $(3.6 \pm 0.6 \text{ nm})$  was higher than WT mice  $(3.0 \pm 0.4 \text{ nm})$  and the differences, although small, were statistically significant (p = 0.030). To further ascertain the impact of DDR1 on collagen fibril ultrastructure, AFM analysis was also conducted on collagen fibrils reconstituted in vitro in the presence or absence of recombinant DDR1-Fc. Collagen fibrils lacking DDR1-Fc exhibited a distinct D-periodicity and the depth of the gap region could be ascertained from the AFM topographic images (Fig. 7;  $1.6 \pm 0.4$  nm). In contrast, the majority of fibrils formed in the presence of DDR1-Fc exhibited a flat topography with no discernible banded structure (Fig. 7).

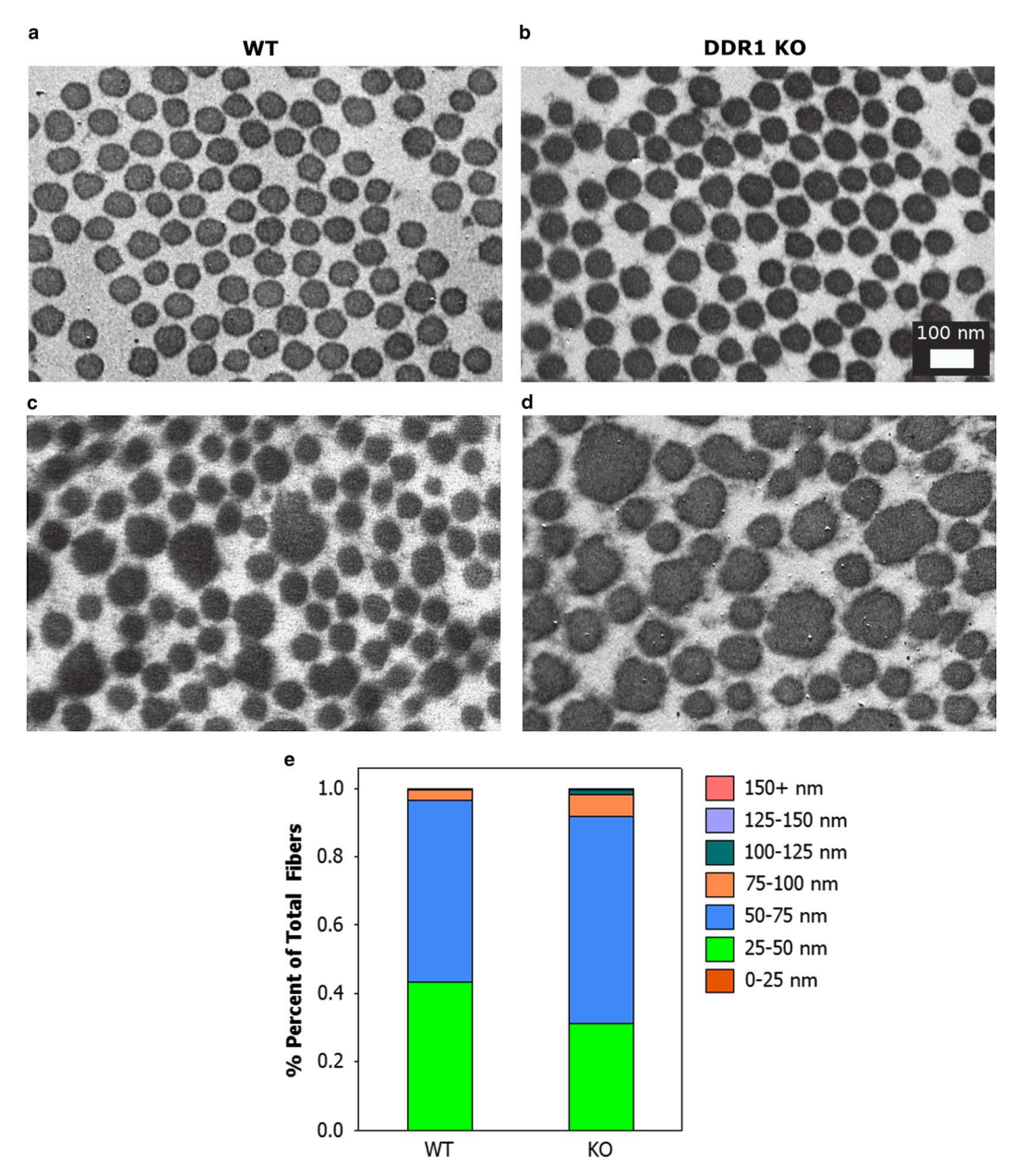


**Figure 4.** Collagen fibril diameter distribution in the mouse tunica adventitia. Representative transmission electron microscopy images of typical collagen fibril cross-sections from (a) discoidin domain receptor 1 (DDR1) knock-out (KO) and (b) wild-type (WT) are displayed. In addition to regular fibrils, both genotypes exhibited large irregular-shaped collagen fibrils ( $\mathbf{c}$ , $\mathbf{d}$ ), which made up <10% of the total fibrils measured and were only observed near the adventitia-media interface. Scale bar is 100 nm. **e:** Average percentage of fibrils in each diameter range across eight mice of each genotype. The  $\chi^2$  test showed that the percent of fibrils >50 nm was significantly higher in the DDR1 KO mice (p < 0.0001).

The fibril orientation with respect to the fast-scan axis in our AFM images was random for both *in vivo* and *in vitro* samples. To rule out the effect of fibril orientation on measured D-periods, we analyzed fibrils at a fixed fibril orientation (±15°) for each WT/KO littermate pair. As shown in Figure 8, the mean D-depth per fibril was higher for DDR1 KO mice irrespective of fibril orientation for six out of the eight pairs examined. The depth of D-periods of *in vitro* created collagen fibrils was identical at the two different fibril orientations measured. No significant

differences were observed in the depths of D-periods when measurements were repeated using different probes from the same lot on the same sample (supporting information).

# Discussion

DDR1 KO mice utilized in this study were generated by homologous recombination (by replacing exons 1–3). A similar approach (replacing exons 1–17) was used to

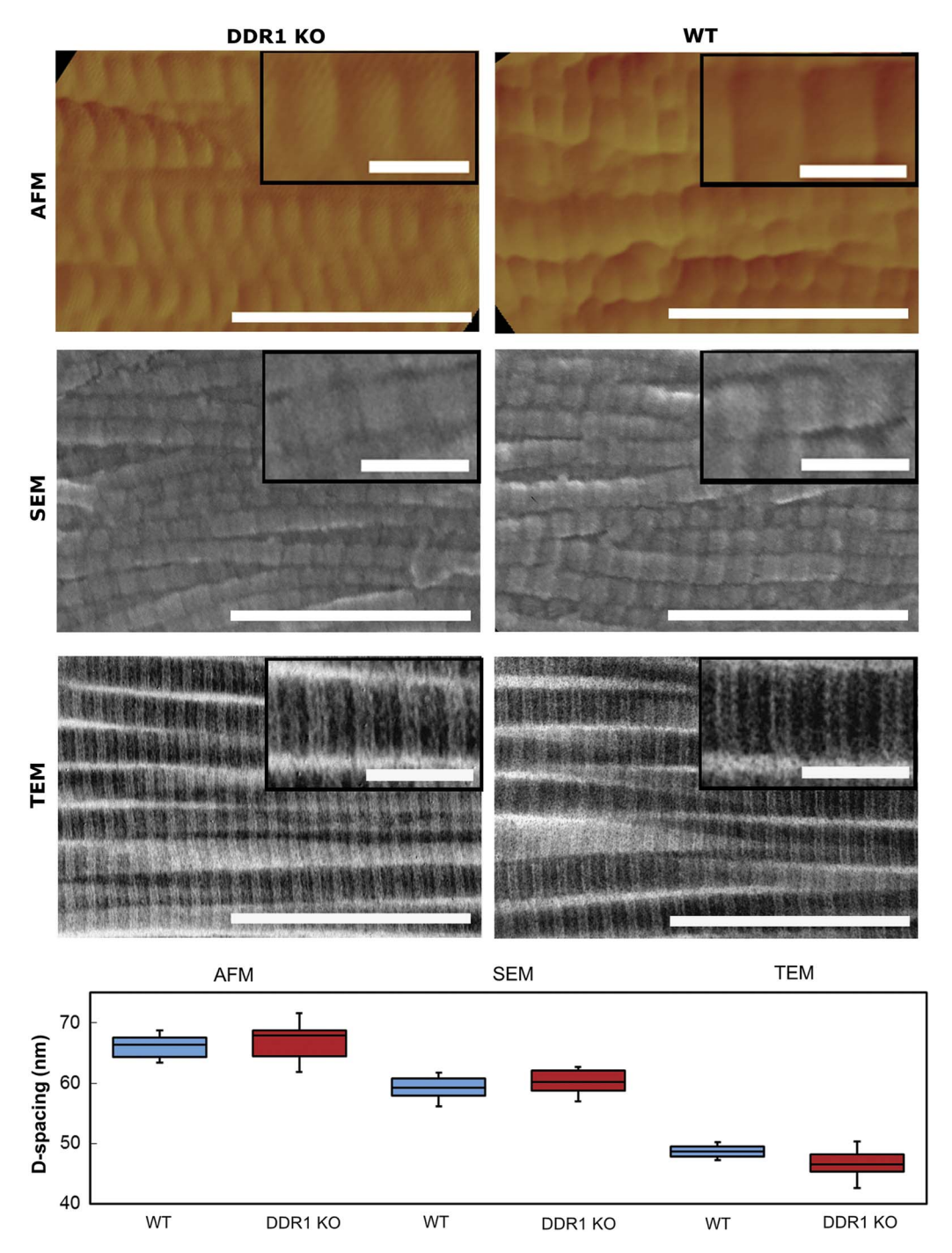


**Figure 5.** Length of D-periods in collagen fibrils from discoidin domain receptor 1 (DDR1) knock-out (KO) mice examined by atomic force microscopy (AFM), scanning electron microscopy (SEM), and transmission electron microscopy (TEM). Representative AFM (amplitude), SEM, and TEM images of adventitial collagen fibrils from DDR1 KO and wild-type (WT) aortas are displayed. Higher magnification images are shown as insets. Boxplots are shown for each imaging technique. Scale bar is 225 nm (inset scale bars are 100 nm).

generate DDR1 KO mice by Vogel et al. (2001). Our studies reveal that DDR1 KO mice have increased collagen deposition in the adventitia. These observations are consistent with increased collagen deposition observed in the mammary gland (Vogel et al., 2001) and in atherosclerotic plaques (Franco et al., 2008, 2010) of DDR1 KO mice from the Vogel model. It is interesting to note that despite sharing the same

binding location on collagen, the role of SPARC (secreted protein acidic and rich in cysteine), another CBP, is contrary to that of DDR1 in regulating collagen. Deletion of SPARC reduces collagen deposition (Bradshaw et al., 2003), whereas deletion of DDR1 increases collagen deposition. This may be partly explained by the fact that even though DDRs and SPARC share the same amino acid binding sequence on

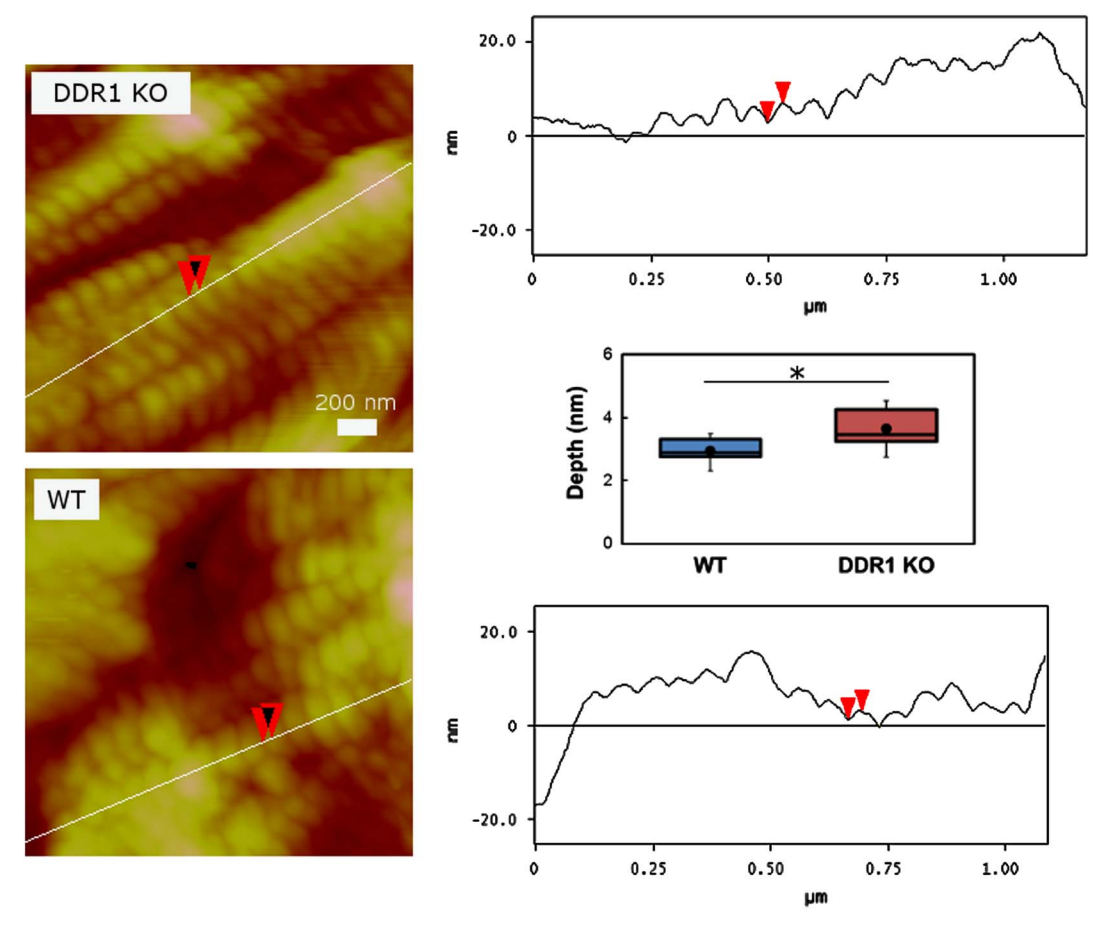


**Figure 6.** Increased D-period depth in collagen fibrils from discoidin domain receptor 1 (DDR1) knock-out (KO) mice. Representative atomic force microscopy topographic images from the adventitia of DDR1 KO and wild-type (WT) aortas show collagen fibrils. Section profiles, measured along the axis of the fibril, are shown next to the corresponding image. Boxplots exhibit mean depth of D-periodicity for each genotype. Collagen fibrils from DDR1 KO mice exhibited a significantly greater depth compared with WT (p = 0.030).

collagen (Giudici et al., 2008; Xu et al., 2011), they recognize different chains of the collagen triple helix (Brondijk et al., 2012).

Multiple mechanisms may contribute to the increased collagen deposition observed in DDR1 KO mice including altered cell density, collagen synthesis, and collagen fibrillogenesis. In our study, we did not observe a significant difference in the number of adventitial fibroblasts between the two genotypes (data not shown). Previous reports revealed that collagen synthesis is affected by the expression of DDR1. Studies using primary smooth muscle cells have shown that messenger ribonucleic acid (mRNA) levels for collagen types I and III were significantly higher in DDR1 KO cells compared with WT cells (Franco et al., 2008; Roig et al., 2010). Overexpression (by transient transfection) of DDR1 in human smooth muscle cells induced a significant decrease in collagen type I mRNA, which was accompanied by a similar decrease at the protein level (Ferri et al., 2004). Further, our in vitro studies have elucidated how DDR1 (and DDR2) expression inhibits collagen fibrillogenesis (Blissett et al., 2009; Flynn et al., 2010). Thus, the increase in adventitial collagen observed in the DDR1 KO mice could be caused by DDR1 suppressing collagen synthesis and/or fibrillogenesis.

Our fibril diameter analysis revealed a higher percentage of larger collagen fibrils (>50 nm diameter) in DDR1 KO adventitia as compared with WT. This observation is consistent with our studies where overexpression of DDR1 ECD in cultured cells resulted in reduced fibril diameters (Flynn et al., 2010). However, a milder effect of DDR1 on fibril diameters was observed in vivo, as compared with our cell culture studies. This could be due to the fact that the level of endogenous DDR1 present in WT murine aorta is not as high as that in our DDR1 ECD transfected cells. This explanation can be further affirmed by our previous study where the expression level of DDR2 ECD in cells inversely correlated with fibril diameter (Blissett et al., 2009). Variation in adventitial collagen fibril diameter has also been reported in mice lacking other genes. These include an increased range of fibril diameters in the biglycan KO mice (Heegaard et al., 2007), and a higher percentage of larger fibrils in mice lacking collagen III (Liu et al., 1997). Besides fibrils with circular cross-sections, we also observed irregularly shaped collagen fibrils at the adventitia-media interface in both the DDR1 KO and WT mice. Irregular fibril cross-sections and collagen "flowers" have also been observed in healthy human aorta media,

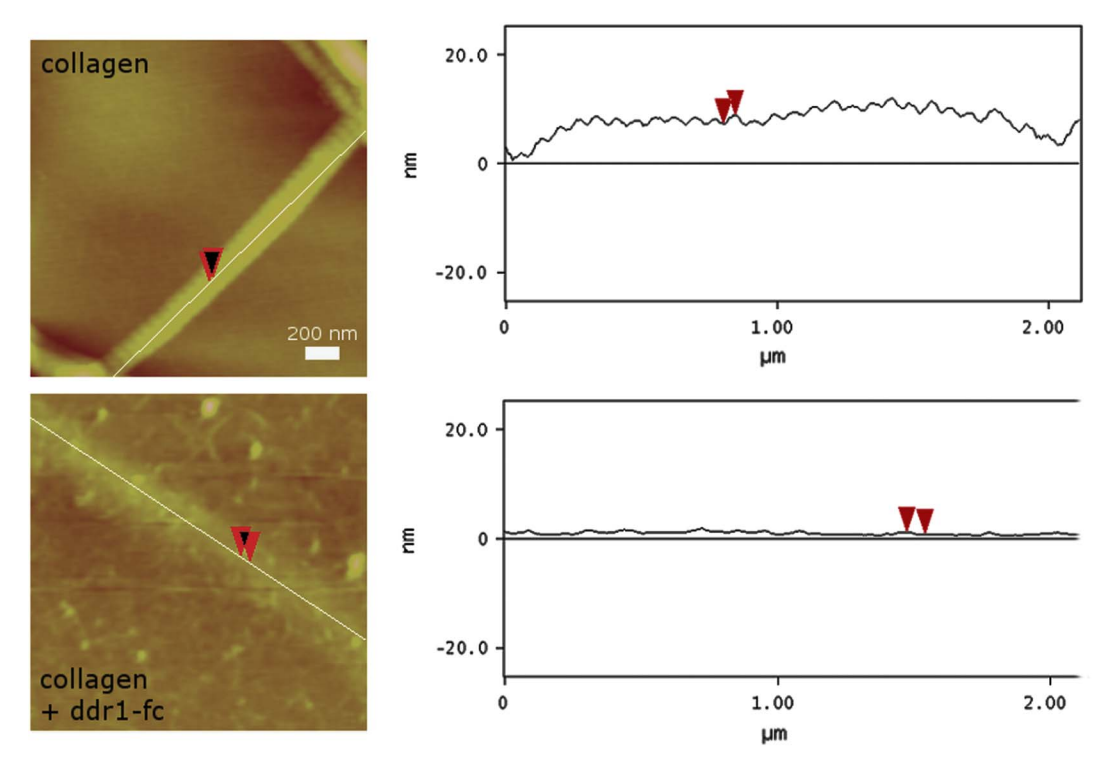


**Figure 7.** Representative atomic force microscopy (AFM) topographic images of collagen fibrils reconstituted in the absence and presence of discoidin domain receptor 1 (DDR1)-Fc. Collagen fibrils with DDR1-Fc exhibited no banded structure or measurable D-period depth. Line profiles of a collagen fibril are displayed adjacent to the corresponding AFM images. Scale bar is 200 nm.

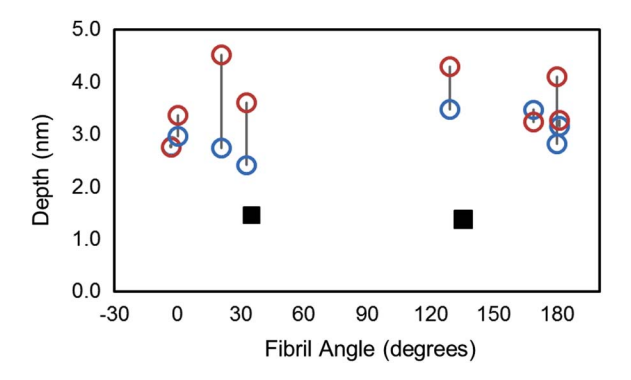


Figure 8. Effect of fibril orientation on the D-period depth. Fibrils from atomic force microscopy images were selected for each wild-type/knock-out (WT/KO) littermate pair, which were at identical orientations ( $\pm 15^{\circ}$ ) for that set. WT/KO littermate pairs are indicated by a gray line connecting the discoidin domain receptor 1 KO (red circle) and the WT (blue circle). The fibril D-depth is plotted as a function of the mean fibril orientation for that pair. D-period depth from *in vitro* reconstituted collagen is shown as black squares.

particularly near the adventitia (Ishii & Asuwa, 1996; Dingemans et al., 2000).

Our results show no difference in the mean length of D-periodicity present in collagen fibrils from DDR1 KO versus WT mice. These results are consistent with our earlier *in vitro* observations where no changes in the length of

D-periods was found in collagen fibrils reconstituted in the presence of recombinant DDR1-Fc (Agarwal et al., 2007) or those formed by cells expressing DDR1 ECD (Flynn et al., 2010). Our observations are consistent with recent reports elucidating how the evolution of collagen has constrained possible alterations in the length of D-periods in collagen fibrils (Slatter & Farndale, 2015), and how the mean length of D-periods is not significantly altered even in dis eases characterized by collagen mutations (Wallace et al., 2011; Erickson et al., 2013). Only one study has reported collagen fibrils exhibiting a significant alteration in length of D-period in vivo. The D-period length of collagen fibrils, isolated from the tendon of TGFβ-inducible early gene-1 (TIEG1) KO mice and measured by X-ray diffraction, was increased and correlated with a higher disorder in packing of collagen molecules (Gumez et al., 2010). Further studies will be required to understand the conditions and mechanism(s) that may induce alterations in the length of D-periodicity in collagen fibrils.

A marked shrinkage was observed in the length of D-periodicity in our study when comparing different imaging modalities. After glutaraldehyde fixation and air drying, AFM imaging yielded D-periodicity values within range of the standard D-period of 67 nm. After metal coating for SEM, the mean collagen periodicity was decreased to ~60 nm. Furthermore, after ethanol dehydration and epoxy resin embedding for TEM, collagen fibrils exhibited a drastically reduced periodicity of ~47 nm. Such a marked shrinkage in the observed D-periodicity for collagen fibrils in

soft tissue is likely due to dehydration and infiltration procedures (Hulmes et al., 1981), and the specific fixative and resin used for TEM samples (Akhtar, 2012).

The most characteristic feature of an altered ultrastructure of collagen fibrils formed in the absence versus presence of DDR1 was a change in the depth of the D-periods (i.e., the difference in relative height of the gap and overlap regions in a D-period). Our results show a small but statistically significant increase in the depth of D-periodicity in DDR1 KO adventitia collagen fibrils as compared with their WT littermates. Consistent with these results, in vitro reconstituted collagen fibrils in the presence of recombinant DDR1-Fc had a negligible D-period depth. These results are useful in understanding how the presence of DDR1 resulted in a weakening of D-periodicity in our earlier in vitro studies (Agarwal et al., 2007) employing TEM. We postulate that the presence of DDR1 ECD during collagen fibrillogenesis may affect the packing of collagen molecules in the gap region of the microfibril and thus reduce the relative height difference between the gap and overlap regions. Our efforts to identify if DDR1 ECD remains bound to collagen fibrils in vivo have not been successful, thus far, with the currently available DDR1 antibodies and reagents. We also noted that, in our study, the collagen fibrils reconstituted in vitro exhibited a smaller D-period depth  $(1.6 \pm 0.4 \,\mathrm{nm})$  as compared with collagen fibrils from the WT murine aortic adventitia  $(3.0 \pm 0.4 \text{ nm})$ . Previous reports revealed that D-period depth is dependent on the specific environment in which the collagen fibrils are formed. For instance, D-period depth in bovine (Yamamoto et al., 1997) and human sclera (Yamamoto et al., 2002), and in rat tail tendon (Baselt et al., 1993) was reported to be ~6 nm, whereas those in bovine (Yamamoto et al., 1997) and human corneas (Yamamoto et al., 2002) were ~2-3 nm.

Taken together our results demonstrate that deficiency of DDR1 results in increased collagen deposition accompanied by changes in collagen fibril ultrastructure in the murine adventitia. Increased interstitial or perivascular (adventitial) collagen deposition is found in cardiovascular pathologies such as hypertrophic cardiomyopathy (Shirani et al., 2000) or arterial remodeling (Durmowicz et al., 1994). It is possible that alterations in the expression level of collagen receptors like DDR1, along with changes in the collagen ultrastructure, exist in these pathologies. An altered collagen ultrastructure may also affect cell-matrix interactions, matrix mineralization, and mechanical properties of the underlying tissues. In this regard, it is interesting to note that the proliferation and migration of smooth muscle cells with/out DDR1 is noted to depend on the ECM microenvironment (Franco et al., 2010). Further mineralization of the ECM was directly correlated with expression of DDR1 in both in vitro (Flynn et al., 2010) and in vivo (Ahmad et al., 2009) studies. Collagen fibrils formed in the presence of DDR2 showed reduced persistence length (Sivakumar & Agarwal, 2010). Characterizing the collagen fibril ultrastructure may thus provide novel insights into functional properties of the ECM.

# ACKNOWLEDGMENTS

The authors would like to acknowledge Alex Dibartola and Dr. Steven Lower for assistance and use of their Bioscope Resolve for AFM probe characterization. The authors thank Sarah Chen for contributing to collagen fibril diameter measurements. Paraffin embedding of aortas and trichrome staining were performed by the OSU Comprehensive Cancer Center's Comparative Pathology & Mouse Phenotyping Shared Resource (CPMPSR). The CPMPSR is partially supported by the Cancer Center Support Grant - P30 CA016058. This work was supported in part by the NSF CMMI 1201111 and a seed award by the NIH CTSA Grant (UL1TR001070) to G.A. and by an AHA predoctoral fellowship to J.R.T.

# REFERENCES

- AGARWAL, G., MIHAI, C. & ISCRU, D.F. (2007). Interaction of discoidin domain receptor 1 with collagen type 1. J Mol Biol 367, 443-455.
- AHMAD, P.J., TRCKA, D., XUE, S., FRANCO, C., SPEER, M.Y., GIACHELLI, C.M. & Bendeck, M.P. (2009). Discoidin domain receptor-1 deficiency attenuates atherosclerotic calcification and smooth muscle cellmediated mineralization. Am J Pathol 175, 2686-2696.
- AKHTAR, S. (2012). Effect of processing methods for transmission electron microscopy on corneal collagen fibrils diameter and spacing. Microsc Res Tech 75, 1420-1424.
- Ameye, L., Aria, D., Jepsen, K., Oldberg, A., Xu, T. & Young, M.F. (2002). Abnormal collagen fibrils in tendons of biglycan/ fibromodulin-deficient mice lead to gait impairment, ectopic ossification, and osteoarthritis. FASEB J 16, 673-680.
- Baselt, D.R., Revel, J.P. & Baldeschwieler, J.D. (1993). Subfibrillar structure of type I collagen observed by atomic force microscopy. *Biophys J* **65**, 2644–2655.
- BHATNAGAR, R.S., QIAN, J.J. & GOUGH, C.A. (1997). The role in cell binding of a beta-bend within the triple helical region in collagen alpha 1 (I) chain: Structural and biological evidence for conformational tautomerism on fiber surface. J Biomol Struct Dyn 14, 547-560.
- BLISSETT, A.R., GARBELLINI, D., CALOMENI, E.P., MIHAI, C., ELTON, T.S. & AGARWAL, G. (2009). Regulation of collagen fibrillogenesis by cell-surface expression of kinase dead DDR2. J Mol Biol 385, 902-911.
- Bradshaw, A.D., Baicu, C.F., Rentz, T.J., Van Laer, A.O., BONNEMA, D.D. & ZILE, M.R. (2010). Age-dependent alterations in fibrillar collagen content and myocardial diastolic function: role of SPARC in post-synthetic procollagen processing. Am J Physiol Heart and Circ Physiol 298, H614-H622.
- Bradshaw, A.D., Puolakkainen, P., Dasgupta, J., Davidson, J.M., WIGHT, T.N. & HELENE SAGE, E. (2003). SPARC-null mice display abnormalities in the dermis characterized by decreased collagen fibril diameter and reduced tensile strength. J Invest Dermatol **120**, 949-955.
- Brondijk, T.H.C., Bihan, D., Farndale, R.W. & Huizinga, E.G. (2012). Implications for collagen I chain registry from the structure of the collagen von Willebrand factor A3 domain complex. Proc Natl Acad Sci U S A 109, 5253-5258.
- Chakravarti, S., Magnuson, T., Lass, J.H., Jepsen, K.J., LaMantia, C. & CARROLL, H. (1998). Lumican regulates collagen fibril assembly: skin fragility and corneal opacity in the absence of lumican. J Cell Biol 141, 1277-1286.

- CHAKRAVARTI, S., PETROLL, W.M., HASSELL, J.R., JESTER, J.V., LASS, J.H., PAUL, J. & BIRK, D.E. (2000). Corneal opacity in lumican-null mice: defects in collagen fibril structure and packing in the posterior stroma. Invest Ophthalmol Visual Sci 41, 3365-3373.
- CHEN, H., LIU, Y., SLIPCHENKO, M. & ZHAO, X. (2011). The layered structure of coronary adventitia under mechanical load. Biophys J 101, 2555-2562.
- CHENG, J. & STOILOV, I. (2013). A fiber-based constitutive model predicts changes in amount and organization of matrix proteins with development and disease in the mouse aorta. Biomech Model Mechanobiol 12, 497-510.
- Danielson, K.G., Baribault, H., Holmes, D.F., Graham, H., KADLER, K.E. & IOZZO, R.V. (1997). Targeted disruption of decorin leads to abnormal collagen fibril morphology and skin fragility. J Cell Biol 136, 729-743.
- DINGEMANS, K.P., TEELING, P., LAGENDIJK, J.H. & BECKER, A.E. (2000). Extracellular matrix of the human aortic media: An ultrastructural histochemical and immunohistochemical study of the adult aortic media. Anat Rec 258, 1-14.
- Dupuis, L.E., Berger, M.G., Feldman, S., Doucette, L., FOWLKES, V., CHAKRAVARTI, S., THIBAUDEAU, S., ALCALA, N.E., Bradshaw, A.D. & Kern, C.B. (2015). Lumican deficiency results in cardiomyocyte hypertrophy with altered collagen assembly. J Mol Cell Cardiol 84, 70-80.
- Durmowicz, A.G., Parks, W.C., Hyde, D.M., Mecham, R.P. & STENMARK, K.R. (1994). Persistence, re-expression, and induction of pulmonary arterial fibronectin, tropoelastin, and type I procollagen mRNA expression in neonatal hypoxic pulmonary hypertension. Am J Pathol 145, 1411–1420.
- ERICKSON, B., FANG, M., WALLACE, J.M., ORR, B.G., LES, C.M. & BANASZAK HOLL, M.M. (2013). Nanoscale structure of type I collagen fibrils: Quantitative measurement of D-spacing. Biotechnol J 8, 117–126.
- Farndale, R.W., Lisman, T., Bihan, D., Hamaia, S., Smerling, C.S., Pugh, N., Konitsiotis, A., Leitinger, B., de Groot, P.G., Jarvis, G.E. & RAYNAL, N. (2008). Cell-collagen interactions: the use of peptide toolkits to investigate collagen-receptor interactions. Biochem Soc Trans 36, 241-250.
- Ferri, N., Carragher, N.O. & Raines, E.W. (2004). Role of discoidin domain receptors 1 and 2 in human smooth muscle cell-mediated collagen remodeling: Potential implications in atherosclerosis and lymphangioleiomyomatosis. Am J Pathol **164**, 1575-1585.
- Flynn, L.A., Blissett, A.R., Calomeni, E.P. & Agarwal, G. (2010). Inhibition of collagen fibrillogenesis by cells expressing soluble extracellular domains of DDR1 and DDR2. J Mol Biol 395, 533-543.
- Fomovsky, G., Rouillard, A. & Holmes, J. (2012). Regional mechanics determine collagen fiber structure in healing myocardial infarcts. J Mol Cell Cardiol 52, 1083-1090.
- Franco, C., Ahmad, P.J., Hou, G., Wong, E. & Bendeck, M.P. (2010). Increased cell and matrix accumulation during atherogenesis in mice with vessel wall-specific deletion of discoidin domain receptor 1. Circ Res 106, 1775-1783.
- Franco, C., Britto, K., Wong, E., Hou, G., Zhu, S.-N., Chen, M., CYBULSKY, M.I. & BENDECK, M.P. (2009). Discoidin domain receptor 1 on bone marrow-derived cells promotes macrophage accumulation during atherogenesis. Circ Res 105, 1141-1148.
- Franco, C., Hou, G., Ahmad, P.J., Fu, E.Y.K., Koh, L., Vogel, W.F. & Bendeck, M.P. (2008). Discoidin domain receptor 1 (ddr1) deletion decreases atherosclerosis by accelerating matrix accumulation and reducing inflammation in low-density lipoprotein receptor-deficient mice. CircRes 102, 1202-1211.

- Fu, H.-L., Sohail, A., Valiathan, R.R., Wasinski, B.D., Kumarasiri, M., Mahasenan, K.V., Bernardo, M.M., Tokmina-Roszyk, D., FIELDS, G.B., MOBASHERY, S. & FRIDMAN, R. (2013). Shedding of discoidin domain receptor 1 by membrane-type matrix metalloproteinases. J Biol Chem 288, 12114-12129.
- GHAZANFARI, S. & DRIESSEN-MOL, A. (2012). A comparative analysis of the collagen architecture in the carotid artery: Second harmonic generation versus diffusion tensor imaging. Biochem Biophys Res Commun 426, 54-58.
- GIUDICI, C., RAYNAL, N., WIEDEMANN, H., CABRAL, W.A., MARINI, J.C., TIMPL, R., BÄCHINGER, H.P., FARNDALE, R.W., SASAKI, T. & TENNI, R. (2008). Mapping of SPARC/BM-40/osteonectinbinding sites on fibrillar collagens. J Biol Chem 283, 19551-19560.
- Gumez, L., Bensamoun, S.F., Doucet, J., Haddad, O., Hawse, J.R., Subramaniam, M., Spelsberg, T.C. & Pichon, C. (2010). Molecular structure of tail tendon fibers in TIEG1 knockout mice using synchrotron diffraction technology. J Appl Physiol **108**, 1706-1710.
- HECHLER, B., NONNE, C., ECKLY, A., MAGNENAT, S., RINCKEL, J.-Y., Denis, C.V., Freund, M., Cazenave, J.-P., Lanza, F. & Gachet, C. (2010). Arterial thrombosis: Relevance of a model with two levels of severity assessed by histologic, ultrastructural and functional characterization. J Thromb Haemost 8, 173-184.
- HEEGAARD, A.-M., CORSI, A., DANIELSEN, C.C., NIELSEN, K.L., JORGENSEN, H.L., RIMINUCCI, M., YOUNG, M.F. & BIANCO, P. (2007). Biglycan deficiency causes spontaneous aortic dissection and rupture in mice. Circulation 115, 2731-2738.
- HERR, A.B. & FARNDALE, R.W. (2009). Structural insights into the interactions between platelet receptors and fibrillar collagen. J Biol Chem 284, 19781-19785.
- Horcas, I., Fernández, R., Gómez-Rodríguez, J.M., Colchero, J., GÓMEZ-HERRERO, J. & BARO, A.M. (2007). WSXM: A software for scanning probe microscopy and a tool for nanotechnology. Rev Sci Instrum 78, 013705.
- Hou, G., Vogel, W. & Bendeck, M.P. (2001). The discoidin domain receptor tyrosine kinase DDR1 in arterial wound repair. J Clin Invest 107, 727-735.
- Hulmes, D.J., Jesior, J.C., Miller, A., Berthet-Colominas, C. & Wolff, C. (1981). Electron microscopy shows periodic structure in collagen fibril cross sections. Proc Natl Acad Sci U S A 78, 3567-3571.
- ISHII, T. & ASUWA, N. (1996). Spiraled collagen in the major blood vessels. Mod Pathol 9, 843-848.
- JEPSEN, K.J., Wu, F., PERAGALLO, J.H., PAUL, J., ROBERTS, L., EZURA, Y., OLDBERGI, A., BIRK, D.E. & CHAKRAVARTI, S. (2002). A syndrome of joint laxity and impaired tendon integrity in lumican- and fibromodulin-deficient mice. J Biol Chem 277, 35532-35540.
- Kyriakides, T.R., Zhu, Y.H., Smith, L.T., Bain, S.D., Yang, Z., LIN, M.T., DANIELSON, K.G., IOZZO, R.V., LAMARCA, M., McKinney, C.E., Ginns, E.I. & Bornstein, P. (1998). Mice that lack thrombospondin 2 display connective tissue abnormalities that are associated with disordered collagen fibrillogenesis, an increased vascular density, and a bleeding diathesis. J Cell Biol 140, 419-430.
- LIU, X., WU, H., BYRNE, M., KRANE, S. & JAENISCH, R. (1997). Type III collagen is crucial for collagen I fibrillogenesis and for normal cardiovascular development. Proc Natl Acad Sci USA 94, 1852-1856.
- Manabe, I., Shindo, T. & Nagai, R. (2002). Gene expression in fibroblasts and fibrosis: involvement in cardiac hypertrophy. Circ Res 91, 1103-1113.

- Norris, R.A., Damon, B., Mironov, V., Kasyanov, V., Ramamurthi, A., Moreno-Rodriguez, R., Trusk, T., Potts, J.D., Goodwin, R.L., DAVIS, J., HOFFMAN, S., WEN, X., SUGI, Y., KERN, C.B., MJAATVEDT, C.H., Turner, D.K., Oka, T., Conway, S.J., Molkentin, J.D., FORGACS, G. & MARKWALD, R.R. (2007). Periostin regulates collagen fibrillogenesis and the biomechanical properties of connective tissues. J Cell Biochem 101, 695-711.
- Orgel, J.P.R.O., IRVING, T.C., MILLER, A. & WESS, T.J. (2006). Microfibrillar structure of type I collagen in situ. Proc Natl Acad Sci U S A 103, 9001-9005.
- Orgel, J.P.R.O., San Antonio, J.D. & Antipova, O. (2011). Molecular and structural mapping of collagen fibril interactions. Connect Tissue Res 52, 2-17.
- RENTZ, T.J., POOBALARAHI, F., BORNSTEIN, P., SAGE, E.H. & Bradshaw, A.D. (2007). SPARC regulates processing of procollagen I and collagen fibrillogenesis in dermal fibroblasts. J Biol Chem 282, 22062-22071.
- Roig, B., Franco-Pons, N., Martorell, L., Tomàs, J., Vogel, W.F. & VILELLA, E. (2010). Expression of the tyrosine kinase discoidin domain receptor 1 (DDR1) in human central nervous system myelin. Brain Res 1336, 22-29.
- SHIRANI, J., PICK, R., ROBERTS, W.C. & MARON, B.J. (2000). Morphology and significance of the left ventricular collagen network in young patients with hypertrophic cardiomyopathy and sudden cardiac death. J Am Coll Cardiol **35**, 36–44.
- Shrivastava, A., Radziejewski, C., Campbell, E., Kovac, L., McGlynn, M., Ryan, T.E., Davis, S., Goldfarb, M.P., Glass, D.J., Lemke, G. & YANCOPOULOS, G.D. (1997). An orphan receptor tyrosine kinase family whose members serve as nonintegrin collagen receptors. Mol Cell 1, 25-34.
- SIVAKUMAR, L. & AGARWAL, G. (2010). The influence of discoidin domain receptor 2 on the persistence length of collagen type I fibers. Biomaterials 31, 4802-4808.
- SLACK, B.E., SINIAIA, M.S. & BLUSZTAJN, J.K. (2006). Collagen type I selectively activates ectodomain shedding of the discoidin domain receptor 1: involvement of Src tyrosine kinase. J Cell Biochem 98, 672-684.
- SLATTER, D.A. & FARNDALE, R.W. (2015). Structural constraints on the evolution of the collagen fibril: Convergence on a 1014-residue COL domain. Open Biol 5, 140220.

- Sugita, S. & Matsumoto, T. (2013). Heterogeneity of deformation of aortic wall at the microscopic level: Contribution of heterogeneous distribution of collagen fibers in the wall. Biomed Mater Eng 23, 447-461.
- Svensson, L., Aszódi, A., Reinholt, F.P., Fässler, R., Heinegård, D. & OLDBERG, A. (1999). Fibromodulin-null mice have abnormal collagen fibrils, tissue organization, and altered lumican deposition in tendon. J Biol Chem 274, 9636-9647.
- SWEENEY, S.M., ORGEL, J.P., FERTALA, A., McAULIFFE, J.D., TURNER, K.R., DI LULLO, G.A., CHEN, S., ANTIPOVA, O., PERUMAL, S., Ala-Kokko, L., Forlino, A., Cabral, W.A., Barnes, A.M., Marini, J.C. & SAN ANTONIO, J.D. (2008). Candidate cell and matrix interaction domains on the collagen fibril, the predominant protein of vertebrates. J Biol Chem 283, 21187-21197.
- Vogel, W., Gish, G.D., Alves, F. & Pawson, T. (1997). The discoidin domain receptor tyrosine kinases are activated by collagen. Mol Cell 1, 13-23.
- Vogel, W.F. (2002). Ligand-induced shedding of discoidin domain receptor 1. FEBS Lett 514, 175-180.
- Vogel, W.F., Aszódi, A., Alves, F. & Pawson, T. (2001). Discoidin domain receptor 1 tyrosine kinase has an essential role in mammary gland development. Mol Cell Biol 21, 2906-2917.
- Wallace, J.M., Orr, B.G., Marini, J.C. & Holl, M.M.B. (2011). Nanoscale morphology of type I collagen is altered in the Brtl mouse model of Osteogenesis Imperfecta. J Struct Biol 173, 146-152.
- WILLIAMS, D.R., SHIFLEY, E.T., LATHER, J.D. & COLE, S.E. (2014). Posterior skeletal development and the segmentation clock period are sensitive to Lfng dosage during somitogenesis. Dev Biol 388, 159-169.
- Xu, H., Raynal, N., Stathopoulos, S., Myllyharju, J., Farndale, R.W. & Lettinger, B. (2011). Collagen binding specificity of the discoidin domain receptors: Binding sites on collagens II and III and molecular determinants for collagen IV recognition by DDR1. Matrix Biol 30, 16-26.
- Yamamoto, S., Hitomi, J., Sawaguchi, S., Abe, H., Shigeno, M. & Ushiki, T. (2002). Observation of human corneal and scleral collagen fibrils by atomic force microscopy. Jpn J Ophthalmol 46, 496-501.
- Yamamoto, S., Hitomi, J., Shigeno, M., Sawaguchi, S., Abe, H. & USHIKI, T. (1997). Atomic force microscopic studies of isolated collagen fibrils of the bovine cornea and sclera. Arch Histol Cytol **60**, 371-378.